Influence of Hydrocarbon Tail Structure on Quinone Binding and Electron-Transfer Performance at the Q_A and Q_B Sites of the Photosynthetic Reaction Center Protein†

Kurt Warncke,* Marilyn R. Gunner,‡ Barry S. Braun,§ Lianquan Gu,‖ Chang-An Yu,‖ J. Malcolm Bruce,⊥ and P. Leslie Dutton§

The Johnson Research Foundation and Department of Biochemistry and Biophysics, University of Pennsylvania, Philadelphia, Pennsylvania 19104, Department of Biochemistry, Oklahoma State University, Stillwater, Oklahoma 74078, and Department of Chemistry, University of Manchester, Manchester M139PL, U.K.

Received December 27, 1993; Revised Manuscript Received March 29, 1994®

ABSTRACT: Binding free energies of 37 functional replacement quinone cofactors with systematically altered hydrocarbon tail structures have been determined for the Q_A and Q_B redox catalytic sites of the reaction center protein isolated from *Rhodobacter sphaeroides* and solubilized in aqueous and in hexane solutions. The first two and part of the third isoprene units of the 10-unit tail of the native ubiquinone-10 cofactor interact with the protein interior at each site. Contributions of the same tail structures to the binding free energies of quinones at the Q_A and Q_B sites are comparable, suggesting that the binding domains share common features. Comparison of the affinities of a homologous series of 10 *n*-alkyl-substituted ubiquinones resolves the binding forces along the length of the tail binding domain and shows that strong steric constraints oppose accommodation of the tail in its extended conformation. Differences in the contributions of identical tail substituents to ubiquinone– and menaquinone–Q_A site affinities, and tail-induced changes of up to 5-fold in the rates of Q_A site-mediated electron-transfer reactions, suggest that the tail adjusts the position of the quinone ring. Substitution of ubiquinone with the native 10-unit isoprene tail does not alter the affinity for the sites as determined in hexane solution. However, one- and two-isoprene-substituted quinones bind more tightly than analogs substituted with saturated-alkyl tail substituents. The sites therefore exhibit binding specificity for the native isoprene tail structure. Calculations indicate that the binding specificity arises primarily from a lower integrated torsion potential energy in the bound isoprene tails. The results suggest that the *in vivo* tail–protein interaction is designed to deter competitive interference of quinone function by amphiphilic species present in the native membrane.

Quinones that function as mediators of vectoral electron and proton transport in photosynthetic and respiratory electron transport chains are amphiphilic molecules composed of a relatively polar quinone ring, or "head group", and an apolar hydrocarbon substituent, or "tail", which is a linear polymer of 6–10 isoprene, 2-methyl-2-butene, units (Crane, 1977; Parson, 1978; Witt, 1979; Wraight, 1979; Crofts & Wraight, 1983; Dutton, 1986). The quinones are localized within the biological membrane, where the majority form a freely diffusing "pool" component. However, it is at quinone binding sites in the membrane redox protein complexes that the sequential electron transfers to and from the bound quinones are coupled directly to the proton binding and release reactions which lead to generation of the transmembrane electrochemical proton gradient (Mitchell, 1961, 1976). The different protein sites promote specialized catalytic function on what is often a common quinone ring structure. For example, quinones bound at the Q_A[1] and Q_B class of quinone redox catalytic sites in photosynthetic reaction center (RC) proteins from bacteria (Kirmaier & Holten, 1987; Feher et al., 1989; Boxer, 1990) and green plant photosystem II (Crofts & Wraight, 1983) display distinct equilibrium binding and electrochemical properties at each site. *In vivo*, the Q_A site quinone functions as an apparently nonexchangeable cofactor. It is reduced to the anionic semiquinone (Q_A^-) in the penultimate electron-transfer step of the light-driven charge separation sequence within the RC protein. In turn, Q_A^- reduces a second quinone molecule bound at the Q_B site. Unlike the Q_A site quinone, the quinone bound at the Q_B site is capable of accepting a second electron (again from Q_A^-), and following binding of two protons to form the hydroquinone species, it rapidly exchanges with the pool (Diner et al., 1984; McPherson et al, 1990; Paddock et al., 1990). In respiratory systems, quinone reduction to the hydroquinone is linked to substrate oxidation at redox catalytic sites in membrane-associated dehydrogenase enzymes (Hederstedt & Ohnishi, 1992). Oxidation of the pool hydroquinone is coupled with vectoral charge separation and proton release on the opposite membrane side at mechanistically distinct catalytic sites located on other membrane redox enzymes (Crofts & Wraight, 1983; Robertson et al., 1990; Ding et al., 1992). Understanding the molecular bases for how protein controls the different equilibrium binding, electrochemical and electron-transfer specifities at these quinone redox catalytic sites is key to

† This work was supported by NSF DMB-88021742 and NIH GM-27309.

* Address correspondence to this author at the Department of Chemistry, Michigan State University, East Lansing, MI 48824.

‡ Present address: Department of Physics, City College of New York, New York, NY 10031.

§ University of Pennsylvania.

‖ Oklahoma State University.

⊥ University of Manchester.

® Abstract published in *Advance ACS Abstracts,* May 15, 1994.

[1] Abbreviations: RC, reaction center, Q_A, primary quinone binding site; Q_B, secondary quinone binding site; UQ_n, ubiquinone (2,3-dimethoxy-5-methyl-1,4-benzoquinone) carrying at the 6-position a tail consisting of *n* isoprene units; MK_n, menaquinone (2-methyl-1,4-naphthoquinone) carrying at the 3-position a tail consisting of *n* isoprene units.

0006-2960/94/0433-7830$04.50/0

obtaining insight into the mechanisms of the efficient capture and stable storage of free energy in photosynthesis and respiration.

The contributions of the protein at the Q_A and Q_B sites to the binding and *in situ* redox catalytic properties of the quinone head group have been investigated in detail in the bacterial RC proteins [Gunner et al., 1985, 1986; Woodbury et al., 1985; Gunner & Dutton, 1989; Moser et al., 1992; Warncke & Dutton, 1993a,b; for reviews, see Feher et al. (1989) and Gunner (1991)], where systematic physical–chemical studies are augmented by knowledge of the structures of the protein and bound cofactors at atomic resolution (Deisenhofer et al., 1985; Michel et al., 1986; Chang et al., 1986, 1991; Allen et al., 1987; Deisenhofer & Michel, 1989). In contrast, a comparable description of the molecular factors governing binding of the tail substituent with protein at the Q_A and Q_B sites, and of the physiological role played by the tail in the direct quinone–protein interaction, has been elusive. This is in part owing to the extreme hydrophobicity of the tail substituent, which has limited study to heterogeneous two-phase solution systems. In these systems, assumptions about the quinone activity coefficients must be made, and distinction between the contributions of solution solvation and direct protein–tail interactions to the binding affinity is not entirely clear. Nevertheless, some progress has been made. Binding studies performed by using purified RC protein incorporated into detergent micelles (Diner et al., 1984; McComb et al., 1990) or artificial phospholipid vesicles (Moser & Dutton, 1987) indicate that, in these systems, the native 10-isoprene-unit tail does not contribute strongly to quinone binding affinity at the Q_A and Q_B sites. However, the effects of synthetic tail substituent structures on electron transport activities mediated by quinones between mitochondrial redox protein complexes in phospholipid–detergent micelles suggest that there are requirements for flexibility in parts of the tail structure that are close to the quinone ring (Yu et al., 1985).

In the present study, we address the factors governing binding of the quinone tail at the Q_A and Q_B sites in the isolated RC protein from *Rhodobacter sphaeroides* by comparing the equilibrium binding free energies of 37 synthetic replacement quinones that have systematically altered hydrocarbon tail structures (for earlier reports, see: Warncke et al., 1987, 1990). The RC protein system is manipulated to achieve accurate determination of binding free energies from homogeneous solution. In aqueous phase binding measurements, the sensitivity of the photochemical assay of functional site occupancy allows work with extremely low RC protein concentrations at detergent concentrations over 50-fold lower than the critical micelle concentration. This also avoids aggregation of the more hydrophobic quinones and stoichiometric binding by extremely tight-binding quinones. Binding free energy measurements are also performed in hydrated hexane solution (Warncke & Dutton, 1993a), by using RC protein solubilized in inverted phospholipid–detergent micelles (Schönfeld et al., 1980). Binding free energies measured in hexane solution provide a clearer estimation of the free energy changes arising from direct, *in situ* interactions between the quinone tail and protein site (Warncke & Dutton, 1993a). This is because the strong interfering contributions of the hydrophobic effect (Tanford, 1980; Sharp et al., 1991) of aqueous desolvation are absent (Warncke & Dutton, 1993a). For many of the synthetic compounds, however, direct protein–tail interactions are sufficiently unfavorable that significant occupancy of the Q_A and Q_B sites cannot be achieved in hexane solution in the absence of the favorable hydrophobic contribution to binding. Therefore, binding free energies for the synthetic tailed quinone compounds are measured in aqueous solution and corrected for their different hydrophobic contributions by subtraction of the separately measured hexane-to-water solvent-transfer free energy of the quinone. This strategy follows the treatment established in head-group binding studies (Warncke & Dutton, 1993a).

The results of this investigation reveal the extent and resolve the position dependence of the free energetic forces acting on the synthetic and native isoprene tail substituents in the Q_A and Q_B sites. The binding free energy analyses, in combination with examination of the quinone tail binding domains in the RC protein X-ray crystallographic structures, yield a detailed molecular level description of the tail–protein interaction. The results also provide insight into the physiological role of the tail–protein interaction.

MATERIALS AND METHODS

Protein Preparation. RC protein from *Rb. sphaeroides* strain R-26 was purified by a procedure based on the method of Clayton and Wang (1971). The native UQ_{10} was extracted from the Q_A and Q_B sites according to the procedure of Okamura et al. (1975), as modified by Woodbury et al. (1985). This method removed all UQ_{10} from the Q_B sites and from more than 98% of the Q_A sites. RC protein (50–100 μM) was stored at −70 °C in 10 mM Tris-HCl buffer at pH 8.0 containing 0.1% (4.4 mM) lauryldimethylamine *N*-oxide (LDAO) detergent. RC protein solubilized in hexane solution was prepared essentially as described (Schönfeld et al., 1980), with some modifications (Warncke & Dutton, 1993a). The properties of the RC protein in the hexane system have been described in detail (Schönfeld et al., 1980; Warncke & Dutton, 1993a).

Measurement of Partition Coefficients. Partition coefficients of the quinones [P = concentration in hexane (M)/concentration in water (M)] were determined at 295 ± 2 K by using a reversed-phase HPLC technique (Braun et al., 1986) that was calibrated using literature P values determined by the shake-flask technique (Leo et al., 1971; Hansch & Leo, 1979).

Kinetic Measurements. The amount of $BChl_2^+$ formed following a xenon flash (pulse FWHM = 8 μs) was monitored optically at $T > 273$ K at 605–540 nm using a dual-beam spectrophotometer (Johnson Foundation). The RC protein concentration was 0.1–0.2 μM and flash saturation 90–95%. The millisecond stabilization of $BChl_2^+$ is due to RC protein containing a functional Q_A site cofactor. Kinetic data were acquired with the aid of Computerscope software (RC Electronics, Santa Barbara, CA) run on a personal computer.

Analysis of the Electron-Transfer Kinetics. Determination of the quantum yield for $BChl_2^+$ formation followed the assumptions and methods described in detail by Gunner and Dutton (1989). The rate constant for Q_A^- to $BChl_2^+$ electron transfer (k_{cr}) was obtained by fitting the decay of $BChl_2^+$ signal to a single exponential plus constant function using either in-house or Asystant+ (Macmillan, New York) software. For all quinones, the amplitude of the constant was ≤5% of the total amplitude of $BChl_2^+$ formed, as previously reported for RC protein incorporating quinone head-group replacements at the Q_A site (Woodbury et al., 1985; Gunner et al., 1986) and in native RC protein (Parot et al, 1987; Sebban, 1988) at 295 K.

Q_A Site Binding Measurements and Analysis. Dissociation constants (K_D; molar units, M) of quinones for the Q_A site of

the RC protein diluted from the preparations to assay concentrations of 0.05–0.2 μM in both the hexane and the aqueous (10 mM Tris buffer, pH 8) systems were determined from functional Q_A site occupancy *versus* concentration of added quinone ($T = 295 \pm 2$ K) (Gunner et al., 1985; Gunner, 1988; Warncke & Dutton, 1993a). The occupancy of the Q_A site was given by the amount of the $BChl_2^+Q_A^-$ state. The $BChl_2^+BPh^-$ state formed by the flash has a lifetime of 13 ns at 295 K. Therefore, the assay addresses the dark, preflash equilibrium occupancy without significant interference from additional diffusion-limited occupancy. Optical measurements were performed on a dual-wavelength spectrophotometer (Johnson Foundation) as described (Gunner et al., 1986). Isotherms were fitted using in-house or Asystant+ analysis software, according to the quadratic treatment of a ligand binding to a population of identical noninteracting sites. The standard free energy of binding (M standard state) was obtained from the measured K_D using $\Delta G°_B = RT \ln K_D$.

For quinones with aqueous phase Q_A site K_D values that were lower than the concentration of RC protein used in the routine binding assay (i.e., $K_D < 100$ nM), K_D values were obtained using the following two modifications of the standard procedure: (a) the concentration of RC protein was lowered to 7–15 nM and (b) a tight-binding, competitive Q_A site inhibitor was added to the medium to displace the apparent K_D of the tail-substituted quinone to a value greater than that of the RC protein concentration. Suitable for this purpose was 2,7-dimethyl-AQ ($K_D = 20$ nM) because charge recombination of the $Q_A^-BChl_2^+$ state formed with this quinone at 295 K occurs within the microsecond duration of the xenon flash and hence does not interfere with the observation of the $Q_A^-BChl_2^+$ signal from the tailed quinone when it occupies the Q_A site. The true K_D for the quinone was calculated from the apparent K_D for binding in the presence of inhibitor, the known K_D of the inhibitor, and its added concentration. Under these conditions, K_D values in the 10 pM range could be measured reliably.

Q_B Site Binding Measurements and Analysis. K_D values in aqueous solution for the Q_B site were determined from functional occupancy of the Q_B site in RC protein containing approximately one native UQ_{10} at the Q_A site (Okamura et al., 1975) following established methods (Giangiacomo & Dutton, 1989; Giangiacomo, 1990). Briefly, the observed fraction of slow ($k \sim 0.1$ s^{-1}) charge recombination from the $BChl_2^+Q_B^-$ state that is formed when Q_A^- reduces quinone occupying the Q_B was compared with that obtained from simulated extents of Q_B reduction (Giangiacomo & Dutton, 1989; Giangiacomo, 1990). A simulation treatment of the Q_B occupancy is required for the following reasons: (a) the small free energy difference between the $BChl_2^+Q_A^-Q_B$ and $BChl_2^+Q_AQ_B^-$ states ($\Delta G°_{AB}$) leads to nonquantitative reduction of quinone occupying the Q_B site; (b) under subsaturating Q_B site conditions, the millisecond lifetime of Q_A^- allows quinone concentration-dependent, diffusion-controlled binding of solution quinone to the Q_B site that elevates the apparent occupancy above that present in the dark, preflash equilibrium (Giangiacomo & Dutton, 1989; McComb et al., 1990). For the simulations, a diffusion-controlled rate constant for binding at the Q_B site of 5×10^7 M^{-1} s^{-1} was assumed (Giangiacomo & Dutton, 1989) and a value of $\Delta G°_{AB} = -1.8$ kcal/mol for electron transfer between UQ_{10} at the Q_A site and the ubiquinone compounds at the Q_B site was assumed that is equal to that for $UQ_{10,A}$ to $UQ_{10,B}$ electron transfer in the native system (Giangiacomo & Dutton, 1989).

Determination of K_D values for isoprene-substituted ubiquinones at the Q_B site with RC protein in hexane solution by this method was not possible because the native UQ_{10} is bound too weakly to the Q_A site and dissociates in this system (Schönfeld et al., 1980). However, the relative k_D values for isoprenyl-substituted ubiquinones with $n \geq 2$ isoprene units could be estimated from the amount of UQ_n reduced at the Q_B site by UQ_n bound at the Q_A site on the basis of the following assumptions: (a) $\Delta G°_{AB}$ remained the same for all quinones [this could not be confirmed for UQ_0 and UQ_1, which are therefore not considered; see Moser and Dutton (1987) and McComb et al. (1990)]; (b) the fraction of the slow phase ($k_{slow} \sim 0.1$ s^{-1}) of charge recombination, obtained from a fit of the decay of absorbance at 605 minus 540 nm to a two-exponential function, represents the fraction of RC protein in which the $BChl_2^+Q_AQ_B^-$ was formed (McComb et al., 1990); (c) quinone binding at the Q_A and Q_B sites is independent. These assumptions allow the apparent K_D for quinone at the Q_B site ($K_{D,Bapp}$) to be calculated from the known value of the K_D at the Q_A site ($K_{D,A}$) and the observed fraction of the slow phase of charge recombination, given by $f(Q_B) = k_{slow}/[k_{fast} + k_{slow}]$ (where k_{fast} is the rate of charge recombination for the $BChl_2^+Q_A^-$ state in RC protein with no quinone bound at the Q_B site), to be obtained from the following equation, which represents the probability that both the Q_A and Q_B sites are occupied in a single RC protein at a given UQ_n concentration ($[UQ_n]$):

$$1/f(Q_B) = (1 + \{K_{D,A}/[UQ_n]\})(1 + \{K_{D,Bapp}/[UQ_n]\}) \quad (1)$$

Sources of Quinone Compounds. All of the substituted ubiquinone compounds used in these studies were synthesized in the laboratory of C.-A. Yu as described (Yu et al., 1985), with the exception of the isoprene compounds UQ_3–UQ_{10} and MK_1 and MK_2, which were gifts from R. Kaback. The *n*-alkyl-substituted menaquinone and naphthoquinone compounds were synthesized in the laboratory of J. M. Bruce, University of Manchester, U.K.

RESULTS

1. Binding of Isoprene-Substituted Ubiquinone Compounds at the Q_A and Q_B Sites in Aqueous Solution. Values of $\Delta G°_{B,w}$ for the series of isoprene-substituted UQ_0 compounds at the Q_A and Q_B sites are presented in Table 1. Representative binding titration curves are shown in Figure 1. Figure 2 shows changes in ubiquinone Q_A site binding strength that accompany substitution with one to five isoprene units. The first isoprene unit contributes –2.5 kcal/mol to the binding strength, but the next two units contribute less (–2.0 and –1.2 kcal/mol, respectively), until the fourth and fifth units make no contributions to the binding strength. Nearly identical patterns are observed for binding at the Q_B site, as shown in Figure 3. The approximately 2 kcal/mol stronger binding affinity of each quinone at the Q_A site relative to the Q_B site is due primarily to the difference in the interaction strength of the ubiquinone head group.

2. Binding of Isoprene-Substituted Ubiquinone Compounds at the Q_A and Q_B Sites in Hexane Solution. Figure 2 shows that, when binding measurements are performed in hexane solution, isoprene substituent contributions to the ubiquinone–Q_A site interaction are severely attenuated relative to the case where the quinone enters the site from water. Figure 2 shows evidence for interactions between the tail substituents and protein in the favorable –0.4 and –1.3 kcal/mol sequential changes in $\Delta G°_{B,hh}$ for UQ_1 and UQ_2, respectively, and the

Table 1: Equilibrium Binding Parameters for Isoprene-Substituted Ubiquinones and Menaquinones at the Q_A and Q_B Sites Determined in Water and Water-Saturated Hexane Solutions and Quinone Water to Hexane Solvent-Transfer Free Energies

	Q_A site				Q_B site				
isoprene quinone	log $K_{D,w}$[a] (M)	$\Delta G°_{B,w}$ (kcal/mol)	log $K_{D,hh}$[a] (M)	$\Delta G°_{B,hh}$ (kcal/mol)	log $K_{D,w}$[a] (M)	$\Delta G°_{B,w}$ (kcal/mol)	log $K_{D,hh}$[a] vs UQ_2 (M)	$\Delta G°_{B,hh}$ vs UQ_2 (kcal)	$\Delta G°_{tr}$(h/w)[b] (kcal/mol)
ubiquinones									
UQ_0	−5.03 ± 0.17	−6.84	−4.20 ± 0.30	−5.71	−3.82 ± 0.17	−5.20	nd[c]		−0.54
UQ_1	−7.07 ± 0.12	−9.62	−4.72 ± 0.10	−6.42	−6.03 ± 0.31	−8.20	nd		−3.85
UQ_2	−8.57 ± 0.16	−11.7	−5.12 ± 0.30	−6.96	−7.50 ± 0.31	−10.20	[0.0] ± 0.4	[0.0]	−7.34
UQ_3	−9.50 ± 0.19	−12.9	−4.26 ± 0.80	−5.79	−8.24 ± 0.36	−11.20	0.3 ± 0.7	0.4	−10.7
UQ_4	−9.63 ± 0.39	−13.1	−4.60 ± 0.40	−6.26	−8.68 ± 0.27	−11.80	0.3 ± 0.4	0.4	−14.5
UQ_5	−9.24 ± 0.60	−12.6	−5.04 ± 0.10	−6.85	−8.01 ± 0.45	−10.90	0.4 ± 0.4	0.5	
UQ_6			−4.31 ± 0.40	−5.86			0.3 ± 0.4	0.4	
UQ_7			−4.36 ± 0.40	−5.93			0.5 ± 0.6	0.7	
UQ_8			−4.12 ± 0.40	−5.60			0.5 ± 0.4	0.7	
UQ_9			−4.32 ± 0.60	−5.88			0.3 ± 0.9	0.4	
UQ_{10}			−3.67 ± 0.50	−4.99			0.8 ± 0.4	1.1	
menaquinones									
MK_0	−6.34 ± 0.05	−8.62	−5.05 ± 0.43	−6.86					−2.39
MK_1	−8.40 ± 0.16	−11.4							−6.39
MK_2	−10.6 ± 0.14	−14.5	−4.97	−6.76					−9.77
MK_{10}			−3.48	−4.73					

[a] Standard experimental deviations are derived from the results of at least three binding titration measurements, performed using at least two separate RC protein preparations. Values with no standard deviation represent a single determination. [b] Standard experimental deviations in the determination of log *P* by the HPLC technique are ≤0.10 log units. [c] nd, not determined.

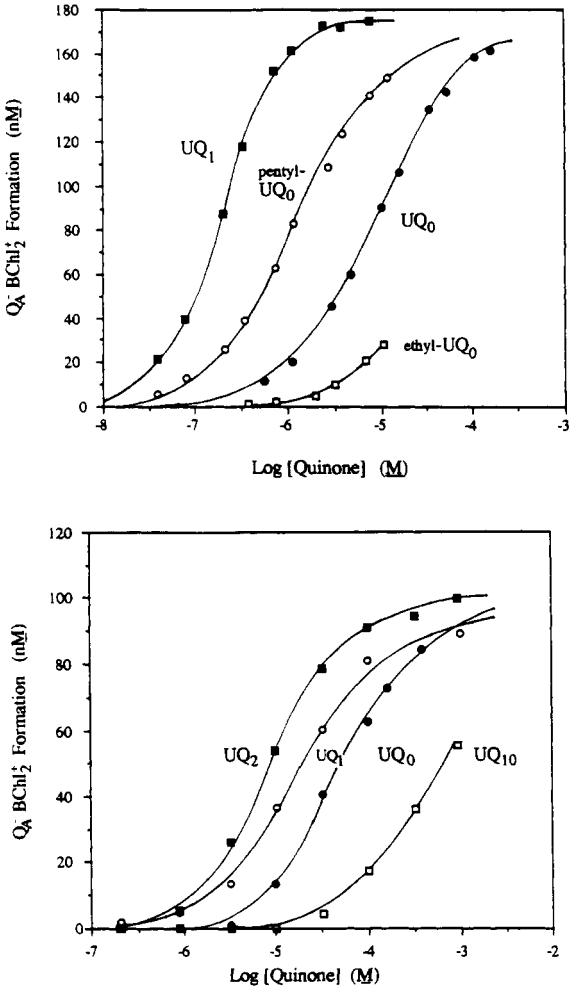

FIGURE 1: Titrations of Q_A site occupancy as a function of the logarithm of the concentration of the indicated quinone present in solution: (A, top) aqueous system; (B, bottom) hydrated hexane system.

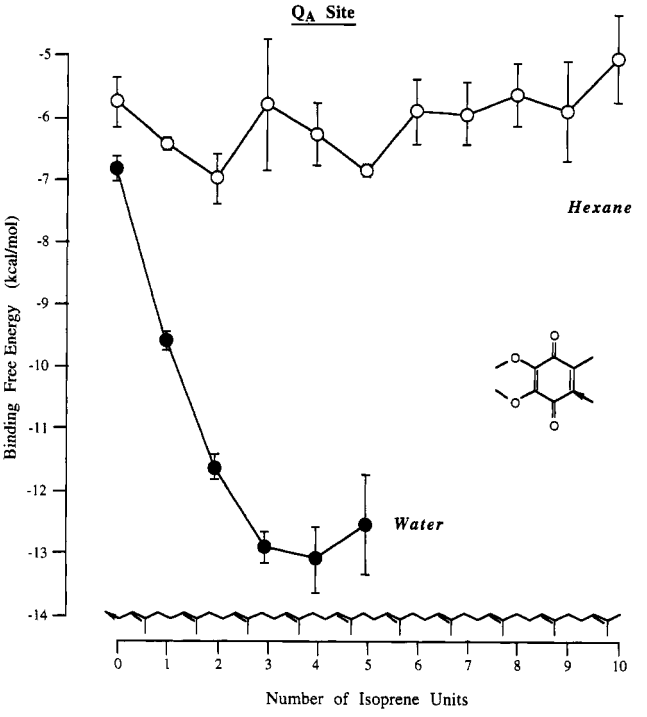

FIGURE 2: Q_A binding free energies of isoprene-substituted ubiquinones in water and in hydrated hexane as a function of the number of isoprene units in the tail.

sharp decline in binding strength of 1.5 kcal/mol for UQ_3. Further minor favorable and unfavorable fluctuations in Q_A site affinity are encountered with each isoprene addition up to 10 units, yielding a binding interaction for UQ_{10} that is somewhat weaker than for UQ_0. Although absolute values of $\Delta G°_{B,hh}$ could not be determined at the Q_B site (see Materials and Methods), Table 1 shows that, relative to the apparent $\Delta G°_{B,hh}$ value of UQ_2, the binding strengths of UQ_3–UQ_{10} are the same to within one experimental standard deviation. This resembles the Q_A site binding behavior.

3. Solvent-Transfer Free Energies of the Quinone Compounds. Values of the water-to-hexane solvent-transfer free energy, $\Delta G°_{tr}$, of the quinones are presented in Table 1. The values are in general agreement with those obtained from comparisons of hydrocarbon chain length and structure effects on $\Delta G°_{tr}$ values in other homologous series (Hansch & Leo, 1979). Methyl-branching introduces a small decrease in the favorability for transfer of the quinone from water to hexane

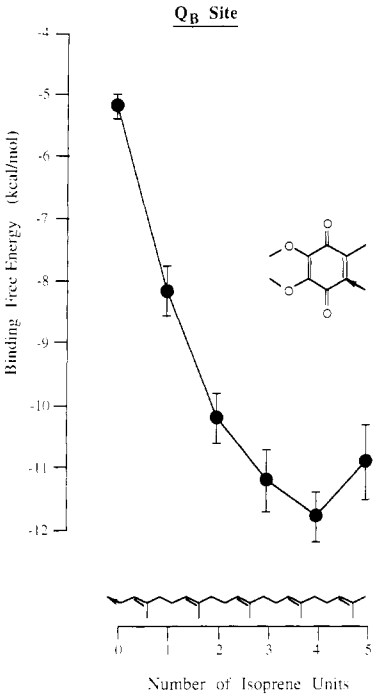

FIGURE 3: Q_B site binding free energies of isoprene-substituted ubiquinones in water as a function of the number of isoprene units in the tail.

of 0.2 kcal/mol per methyl branch relative to the isomeric *n*-alkyl structures. The *n*-alkyl structures display the most favorable $\Delta G°_{tr}$ values on a per carbon atom basis. Formation of a nonconjugated double bond leads to a relatively large decrease in the favorability of water-to-hexane transfer, equivalent to a change in $\Delta G°_{tr}$ of 0.7 kcal/mol per double bond. The effect on $\Delta G°_{tr}$ for formation of conjugated double bonds is nonadditive, as illustrated by comparing the $\Delta G°_{tr}$ values of 2′,4′-hexadienyl-UQ_0 and hexyl-UQ_0. The 2.1 kcal/mol difference in $\Delta G°_{tr}$ is greater than the additive effect of formation of two nonconjugated double bonds (1.5 kcal/mol). The effect is further enhanced for the three conjugated double bonds in 2′,4′,6′-trienyl-UQ_2 relative to dimethyloctanyl-UQ_0, where desaturation increases $\Delta G°_{tr}$ by 4.9 kcal/mol compared with 2.2 kcal/mol for three isolated double bonds.

The structure and length of the hydrocarbon tail strongly influences the solvent-transfer free energy of the quinone. In particular, different configurations of hydrocarbon tails with the same number of carbon atoms lead to significant differences in the quinone $\Delta G°_{tr}$ values. The differences in $\Delta G°_{tr}$ values arise predominantly from differences in the favorable hydrophobic contribution to water-to-hexane partitioning (Tanford, 1980; Sharp et al., 1991). These results clearly demonstrate the necessity of correcting for the hydrophobic solvation contributions to aqueous binding free energies, to obtain a more accurate assessment of the effects of the different tail structures on the direct, *in situ* interactions with protein at the Q_A and Q_B sites. This correction can be achieved by subtraction of the value of $0.78\Delta G°_{tr}$, as previously established (Warncke & Dutton, 1993a).

4. Binding of Ubiquinone Compounds Substituted with Other Tail Structures. a. n-Alkyl-UQ_0 Binding at the Q_A and Q_B Sites. Table 2 presents the $\Delta G°_{B,w}$ values obtained for alkyl-substituted UQ_0 compounds at the Q_A and Q_B sites. The nonuniform contributions of each added methylene unit indicate that the protein environment in the tail binding region is not homogeneous. Figure 4 shows that incremental addition of single methylene carbon groups to the tail leads to a dramatic pattern of changes in the aqueous solvation-corrected binding free energies, $[\Delta G°_{B,w} - 0.78\Delta G°_{tr}]$, for the Q_A and Q_B sites. Comparable trends are displayed at each site. Large unfavorable contributions to binding equivalent to 3.5 kcal/mol are associated with tail extension from methyl to ethyl, which is followed by a smaller additional decrement in affinity on extension to propyl. The extension from propyl to butyl is associated with an increase in affinity (−1.7 kcal/mol), but further addition of methylene units after the fourth leads to a progressive trend toward weakened quinone binding. The net effect of addition of a decyl tail to UQ_0 is a weakening of binding at the Q_A and Q_B sites by over 3 kcal/mol.

b. 2′,4′-Dienylalkyl-UQ_0 Binding at the Q_A Site. As shown in Figure 4, ubiquinones substituted with straight-chain tails that are unsaturated at the 2′- and 4′-positions follow the same general pattern of affinity decreases seen for *n*-alkyl tails of the same carbon atom number but display Q_A site affinities that are roughly −2 kcal/mol stronger. The introduction of the conjugated dienyl structure thus leads to a more favorable interaction with the Q_A site.

c. Binding of Isoprene Analog Compounds at the Q_A and Q_B Sites. Table 2 and Figure 4 present data for the binding of 5- and 10-carbon-atom analogs of the isoprene tails of UQ_1 and UQ_2 at the Q_A and Q_B sites. As shown in Figure 4A, desaturation at the 4′ bond in UQ_2, which would be expected to introduce rigidity in the resulting 2′,4′,6′-trienyl-UQ_2 structure over a length of roughly 7 Å, leads to a weakening of binding at the Q_A site by 1 kcal/mol. In contrast, there is no corresponding weakening of affinity at the Q_B site, where the $[\Delta G°_{B,w} - 0.78\Delta G°_{tr}]$ values of UQ_2 and trienyl-UQ_2 are the same. Binding requirements at the Q_B site therefore are less stringent with regard to accommodation of this rigid tail.

Figure 4 shows that saturation of the isoprene tail double bonds in UQ_1 and UQ_2 leads to a decrease in Q_A and Q_B site binding strength to the same level as the *n*-pentyl- and *n*-decyl-UQ_0 compounds. Therefore, the isoprene-substituted UQ_1 and UQ_2 compounds interact with greater strength at each site relative to analogous saturated alkyl tail structures that incorporate the same number of carbon atoms. This demonstrates that protein at the Q_A and Q_B sites exhibits specificity in the binding interaction with the native isoprene tail structure.

5. Binding of Tail-Substituted Menaquinone and Naphthoquinone Compounds at the Q_A Site. Table 2 presents values of Q_A site $\Delta G°_{B,w}$ and $\Delta G°_{tr}$ for a less complete set of alkyl and isoprene substitutions on the menaquinone head group (2-methyl-1,4-naphthoquinone, MK_0). Parallel measurement of $\Delta G°_{B,w}$ values at the Q_B site by the methods employed here was precluded by the unfavorable Q_A^- to Q_B electron-transfer equilibrium for menaquinones (Giangiacomo & Dutton, 1989). Figure 5 shows that trends in the affinity of MK_0 introduced by these substitutions are similar to those exhibited by the UQ_0 compounds. However, the changes differ in magnitude. These results show that the structure of the head group can influence the observed contributions of the tail to quinone affinity.

Figure 5 also shows that 1,4-naphthoquinones which are disubstituted at the 2,3-positions with *n*-alkyl chains of the same length display dramatically weaker affinity for the Q_A site relative to the corresponding singly substituted MK_0 compounds. The decrease in binding strength becomes more marked with tail extension, with the $\Delta G°_{B,w}$ value for didecyl-MK_0 beyond the limit of detection of occupancy. Accommodation of the bulky, di-*n*-alkyl-substituted quinones in the Q_A site is extremely unfavorable.

Table 2: Q_A and Q_B Site Equilibrium Binding Parameters, Solvent-Transfer Free Energies, and Rate Constants for Charge Recombination for Various Homologous Series of Tail-Bearing Ubiquinones and Menaquinones

	Q_A site		Q_B site			
compound	log $K_{D,w}$[a] (M)	$\Delta G°_{B,w}$ (kcal/mol)	log $K_{D,w}$[a] (M)	$\Delta G°_{B,w}$ (kcal/mol)	$\Delta G°_{tr}$[b] (kcal/mol)	k_{cr}[c] (s^{-1})
ubiquinones						
alkyl-UQ_0						
H-	−5.03 ± 0.17	−6.84	−3.8 ± 0.2	−5.2	−0.54	2.0
methyl-	−6.20 ± 0.11	−8.43	−4.4 ± 0.1	−6.0	−1.24	2.2
ethyl-	−4.32 ± 0.11	−5.88	−2.8 ± 0.2	−3.8	−2.04	2.3
propyl-	−4.32 ± 0.11	−5.88	−3.0 ± 0.2	−4.1	−2.86	2.9
butyl-	−5.29 ± 0.13	−7.19	−3.9 ± 0.2	−5.3	−2.42	3.4
pentyl-	−6.07 ± 0.07	−8.26	−5.4 ± 0.2	−7.3	−4.72	2.9
hexyl-	−6.14 ± 0.04	−8.35	−5.7 ± 0.3	−7.8	−5.74	3.2
heptyl-	−6.69 ± 0.12	−9.10			−6.79	3.4
nonyl-	−7.21 ± 0.00	−9.94	−6.0 ± 0.1	−8.2	−8.79	3.5
decyl-	−7.87 ± 0.04	−10.70	−6.4 ± 0.5	−8.7	−9.79	
2′,4′-dienyl-UQ_0						
hexyl-	−5.99 ± 0.19	−8.15			−4.48	2.9
heptyl-	−6.65 ± 0.20	−9.04			−5.17	2.7
nonyl-	−6.68 ± 0.10	−9.08			−7.07	2.9
other UQ_0						
3′-methyl-butanyl-	−6.00 ± 0.09	−8.16	−5.3 ± 0.1	−7.2	−4.42	3.5
3′,7′-dimethyl-octanyl-	−7.51 ± 0.18	−10.21	nd[d]		−9.75	4.5
2′,4′,6′-trienyl-UQ_2	−6.00 ± 0.39	−8.16	−5.8 ± 0.1	−7.9	−4.88	4.5
menaquinones						
alkyl-MK_0						
H-	−6.34 ± 0.05	−8.62			−2.39	6.7
methyl-	−7.86 ± 0.27	−10.69			−3.54	7.3
ethyl-	−7.40	−10.06			−4.31	9.4
pentyl-	−8.33 ± 0.10	−11.33			−7.34	9.6
decyl-	−9.28 ± 0.26	−12.62			−13.06	9.6
dialkyl-NQ						
2,3-diethyl-	−6.20	−8.43			−5.29	
2,3-dipentyl-	−5.70	−7.75			−8.26	
2,3-didecyl-	>−4.73	>−6.46			−15.23	

[a] Standard experimental deviations are derived from the results of at least three binding titration measurements, performed using at least two separate RC protein preparations. Values with no standard deviation represent a single determination. [b] Standard experimental deviations in the determination of log P by the HPLC technique are ≤0.10 log units. [c] Rate constant for Q_A^- to $BChl_2^+$ charge recombination mediated by the quinone. [d] nd, not determined.

6. Influence of Ubiquinone Tail Length and Structure on Q_A Site-Mediated Electron-Transfer Reaction Rates. a. Charge Separation Reaction. In the terminal step of the light-triggered, charge separation sequence of electron transfers in the RC protein, an electron is transferred from reduced bacteriopheophytin (BPh^-) to the Q_A site quinone. Direct measurement of the rate of this rapid electron transfer (τ = 0.2 ns in the native system) is precluded by the 8-μs width of the actinic xenon flash. However, modifications of the tail in the ubiquinone compounds studied here do not lead to a detectable decrease of the quantum yield for reduction of Q_A from the near unit value characteristic of the native UQ_{10} (Wraight & Clayton, 1973). This indicates that the different tail structures do not diminish the rate of the forward electron transfer from BPh^- to Q_A by more than 10-fold relative to the native rate with UQ_{10} as Q_A (Gunner & Dutton, 1989). Previous quantum yield measurements with quinone head groups at the Q_A site have also demonstrated that the complete absence of a tail structure does not reduce the rate of forward electron transfer by more than 5-fold over the temperature range from 14 to 295 K (Gunner et al., 1982; Gunner & Dutton, 1989). Direct picosecond measurements of the kinetics of electron transfer from BPh^- to tetramethyl-1,4-benzoquinone (1.0×10^9 s^{-1}) and to the native UQ_{10} (4.4×10^9 s^{-1}) at the Q_A site show that the removal of the tail leads to a 4-fold decrease in rate (Laing et al., 1981; Gunner et al., 1982). Further, no significant influence of isoprene tail length on the directly measured rate was observed for *Rb. sphaeroides* RC protein reconstituted with the homologous series of Q_A site cofactors MK_2–MK_8 and UQ_4–UQ_{10} (Schelvis et al., 1992). Therefore, the tail substituents exert relatively small effects on the rates of the BPh^- to Q_A electron transfer that do not influence the unit quantum efficiency characteristic of the native charge separation sequence.

b. Charge Recombination Reaction. Table 2 presents values of the rate constants for the non-native charge recombining electron transfer between Q_A^- and $BChl_2^+$ that proceeds under conditions when the Q_B site is not occupied. The slowest rates of charge recombination are observed for the unsubstituted head groups. Figure 6 shows that the addition of the different tail substituents to UQ_0 and MK_0 leads to qualitatively comparable trends in increased rate. The increases in charge recombination rate observed for substitutions with the native isoprene structure are larger than those for the synthetic tail structures and are complete with the addition of the second isoprene unit. (Ubiquinones: UQ_1, 5.5; UQ_2, 6.7; UQ_3, 6.5; UQ_4, 6.8 s^{-1}. Menaquinones: MK_1, 11.0; MK_2, 12.9; MK_3, 12.8 s^{-1}). The rate exhibited by the native UQ_{10} in native RC protein (7.0 s^{-1}) is only approached by substituted ubiquinones with ≥2 isoprene units. Sequential additions of methylene units in the *n*-alkyl substituent series lead to small increments in rate. Unlike the case for isoprene-substituted quinones, the influence of the alkyl tail appears to be complete with addition of approximately the first five carbon atoms. The rates exhibited by the dienyl-UQ_0 compounds are comparable with those of the corresponding *n*-alkyl-UQ_0 compounds of common tail carbon atom number. These results show that substitution with the tail does not strongly influence the rate of nonphysiological charge recombination reaction and that the modest increases in rate that accompany tail extension are complete with the addition of <10 carbon atoms.

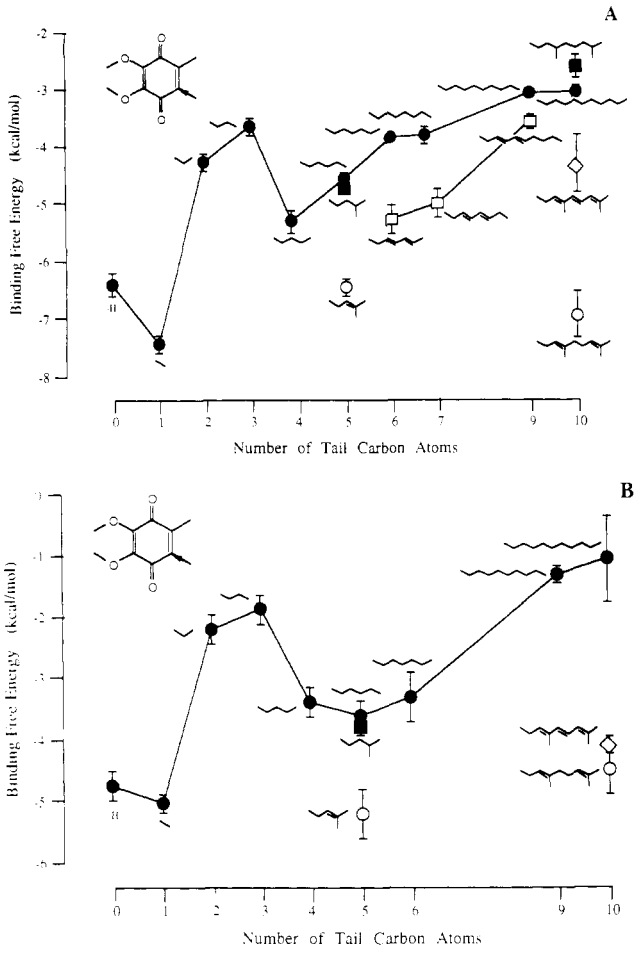

FIGURE 4: Binding free energies of substituted ubiquinones for the Q_A site (A) and Q_B site (B) from hexane solution as a function of the number of carbon atoms in the tail. The ordinate axis represents the binding free energy of the compounds for the Q_A site in hexane solution, obtained from $\Delta G°_{B,hh} = \Delta G°_{B,w} - 0.78\Delta G°_{tr}$ (Warncke & Dutton, 1993a), with the exception of the values for UQ_1 and UQ_2, which are from direct binding measurements in hydrated hexane. The error bars represent the experimental standard deviation of the $\Delta G°_{B,w}$ values.

DISCUSSION

1. Solvation Analysis of Tail-Substituted Quinone Binding at the Q_A Site. Figure 7 shows the difference in the hexane and aqueous solution binding free energies of isoprene-substituted ubiquinones and menaquinones as a function of $-\Delta G°_{tr}$. Quinones substituted with zero, one, and two isoprene units adhere to the same linear relation previously obtained for quinone head groups (Warncke & Dutton, 1993a). The data for UQ_2 and MK_2 extend the range of the correlation obtained for the head groups to $-\Delta G°_{tr}$ values of approximately 10 kcal/mol. These results confirm the validity of using $0.78\Delta G°_{tr}$ to correct $\Delta G°_{B,w}$ to obtain binding free energies for the synthetic tail-substituted quinones which represent entry to the Q_A site from hexane solution.

The results presented in Figure 7 also indicate that hexane molecules do not interact with the tail binding regions at the Q_A site to a degree that would cause competitive interference with binding of the ubiquinones and menaquinones substituted with one and two isoprene units. Competitive interference of hexane with quinone binding would make $\Delta G°_{B,hh}$ more positive and, hence, shift the data points above the fitted line in Figure 7. On initial consideration this is surprising, since hexane molecules are present at a concentration of approximately 7 M in the hexane binding system. However, we

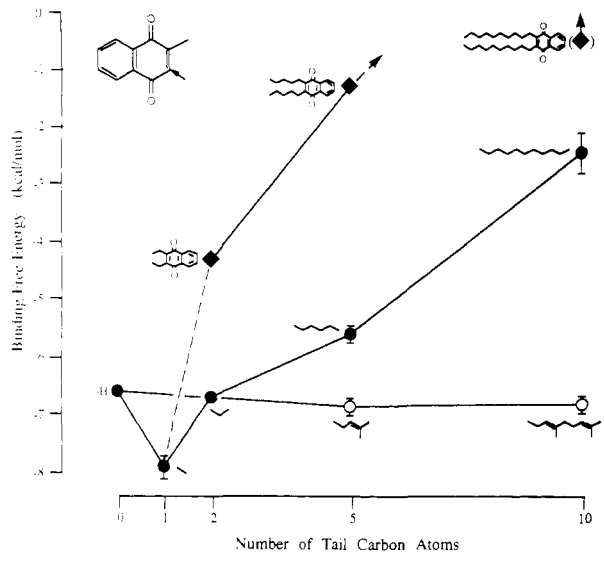

FIGURE 5: Binding free energies of substituted menaquinones and naphthoquinones for the Q_A site from hexane solution as a function of the number of carbon atoms in the tail. The ordinate axis represents the binding free energy of the compounds for the Q_A site in hexane solution, obtained from $\Delta G°_{B,hh} = \Delta G°_{B,w} - 0.78\Delta G°_{tr}$ (Warncke & Dutton, 1993a). The error bars represent the experimental standard deviation of the $\Delta G°_{B,w}$ values.

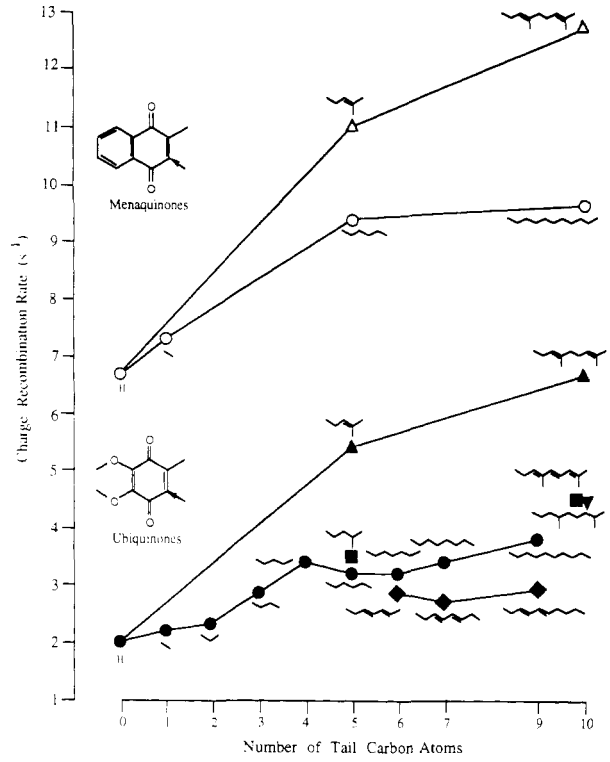

FIGURE 6: Rates of charge recombination mediated by ubiquinone and menaquinone Q_A site cofactors substituted with different tail structures as a function of the number of carbon atoms in the tail substituent. The solid lines connect the *n*-alkyl- and isoprene-substituted quinones.

have found that even in the aqueous system, assisted by the presence of the hydrophobic effect, hexane, octane, 1,5-hexadiene, *trans*-2-nonenal, or the 10- and 15-carbon-atom isoprenols, farnesol and geraniol, do not compete detectably with tailed quinone binding at the Q_A site when present at saturating solution concentrations. Jencks has considered this situation for the case of small substituent fragments that are separated from a parent ligand structure in terms of an inability

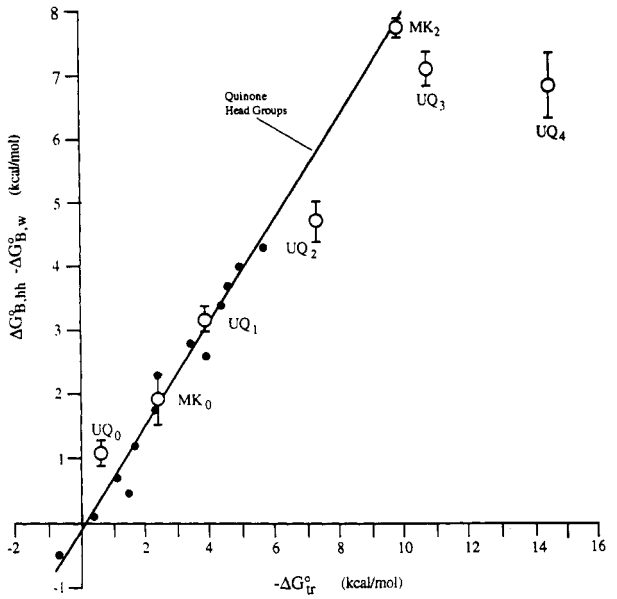

FIGURE 7: Difference between quinone–Q_A site binding free energies determined in hexane and water as a function of the quinone solvent-transfer free energy, $-\Delta G°_{tr}$. The solid line represents the best linear least-squares fit of the data (solid circles) for 14 quinone head groups (small, solid circles) (slope, 0.78; ordinate intercept, –0.13; Warncke & Dutton, 1993a). Open circles represent data for ubiquinone and menaquinone head groups and isoprene-substituted derivatives.

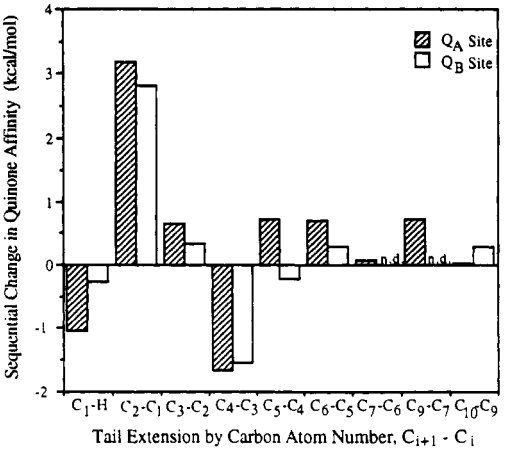

FIGURE 8: Sequential changes in the affinities of ubiquinones for the Q_A and Q_B sites that are associated with extension of the *n*-alkyl tail by individual carbon atom units: (shaded) binding at the Q_A site; (open) binding at the Q_B site. The ordinate axis represents changes in the values of $\Delta G°_{B,hh}$ that are estimated from the relation $\Delta G°_{B,hh} = \Delta G°_{B,w} - 0.78\Delta G°_{tr}$. Data for the differences between heptyl–hexyl and nonyl–heptyl are not presented for Q_B site binding because the K_D value of heptyl-UQ_0 was not determined (n.d.).

of the protein binding energy available from the small substituents to overcome the unfavorable free solution entropy changes necessary for localization in the protein site (Jencks, 1975, 1981). As we will later elaborate, the nondetectable binding of the isolated tail structures also receives a strong contribution from selectively unfavorable interactions within the tail binding domains of the Q_A and Q_B sites. These results indicate that the dominant free energetic contribution to localizing the quinone in the Q_A and Q_B sites is provided by the protein interaction with the quinone head group.

2. Extent of the Tail Binding Domain. Figure 7 shows that the data for UQ_3 and UQ_4 fall below the linear relation. The simplest interpretation of these deviations is that the third and fourth isoprene units are not completely removed from contact with the solvent when the quinone is bound in the Q_A site and thus do not receive a full hydrophobic contribution to $\Delta G°_{B,w}$. If this is true, the deviations in Figure 7 suggest that the Q_A site affinity for UQ_3 receives a partial hydrophobic contribution from the third unit and that there is no hydrophobic contribution to the binding of UQ_4 from the fourth isoprene unit. The comparable pattern of aqueous phase affinity changes at both sites that is shown in Figures 2 and 3 for the isoprene-substituted ubiquinones suggests that these conclusions also apply to the tail interaction at the Q_B site. This analysis suggests that direct interactions between the native isoprene tail and the protein interior extend over only the first two, and part of the third, isoprene units.

3. Resolution of the Factors Governing the Native Tail–Protein Interaction. Figure 8 presents a free energy profile of the sequential changes in the Q_A and Q_B site affinities for ubiquinones as the *n*-alkyl tail substituent is extended. The differences in affinity between the *i*th and the $(i+1)$th member of the homologous series report on new features of the binding domain in the sites encountered by the $(i+1)$th member. Hydrocarbon structures cannot hydrogen bond or form other strong electrostatic or dipolar contacts with the protein (Fersht, 1985). Therefore, unfavorable contributions to binding, represented by the peaks in Figure 8, arise from *in situ* constraints that act to oppose accommodation of the tail in the site. Favorable contributions, represented by the troughs in Figure 8, are determined by occupation of less sterically restricted regions or cavities within the protein binding domains. Figure 8 suggests that less sterically restricted regions are encountered with the addition of the initial methyl group at the Q_A site, in agreement with previous results (Gunner et al., 1985). The smaller methyl group contribution to UQ_0 affinity at the Q_B site suggests that the head-group binding site may be smaller relative to the Q_A site. A relatively uncrowded region at each site is also revealed upon extension of the propyl to the butyl tail. This region may be larger in the Q_B relative to the Q_A site, as evidenced by a further small, favorable affinity increment for extension to the pentyl tail.

Figure 8 also indicates a strong opposition to extension of the tail to two carbon atoms. Comparison of the 2.5 kcal/mol decrease in Q_A site affinity shown in Figure 6 for 2,3-diethyl *versus* 2-ethyl-3-methyl-NQ indicates similar opposition to methyl to ethyl extension from the adjacent, or ortho position on the quinone ring. These results suggest that there is a strong barrier to direct, linear extension of the tail from the quinone ring. The additional small decrease in quinone affinity encountered upon extension of the tail to three carbon atoms may indicate a residual influence of this barrier. Further oppositions to tail accommodation at the Q_A site occur with each further methylene addition after the fourth. The decreased unfavorability of the corresponding contributions at the Q_B site indicates that steric restrictions to accommodation of the tail are less severe than at the Q_A site.

These results demonstrate that, overall, the protein topography acts to oppose the favorable accommodation of the tail substituents in the tail binding domain. This indicates that the flexible *n*-alkyl tails are not bound in the fully extended state that is the average conformation present in solution. The comparable affinities of the 5- and 10-carbon-atom methyl-branched-alkyl and *n*-alkyl ubiquinone compounds suggest that these two tail structures bind in similar regions of the site and experience comparable position-dependent contributions from the protein to affinity. This suggests that the one and two isoprene unit tails, and hence the native isoprene tail, also experience the same position-dependent influences on binding that are resolved in Figure 8.

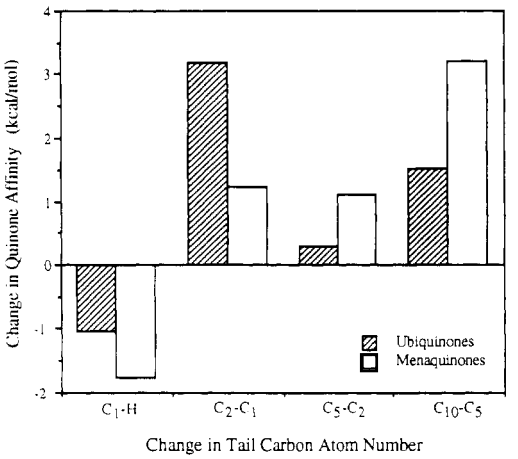

FIGURE 9: Sequential changes in the affinities of ubiquinones and menaquinones for the Q_A site associated with extension of the *n*-alkyl tail substituent by the indicated number of carbon atoms: (shaded) ubiquinones; (open) menaquinones. The ordinate axis represents changes in the values of $\Delta G°_{B,hh}$ that are estimated from the relation $\Delta G°_{B,hh} = \Delta G°_{B,w} - 0.78\Delta G°_{tr}$.

4. Dependence of Tail-Induced Affinity Changes at the Q_A Site on the Quinone Head-Group Structure. Figure 9 shows that different sequential changes in Q_A site affinities result from the same extensions of the *n*-alkyl tail substituent when attached to the UQ_0 and MK_0 head groups. The differences between the two series can be at least partially accounted for by different energetic consequences for alterations in the *in situ* positions of the ubiquinone and menaquinone head groups that are induced cooperatively by tail substitution. If this is true, these results also indicate the following: (a) the *in situ* conformations of the isolated UQ_0 and MK_0 head groups differ from their conformations when substituted with the tail; (b) the free energy changes associated with any readjustments of the quinone ring that are required by substitution with the methyl and ethyl groups are more favorable for the less bulky menaquinone head group relative to the ubiquinone head group. Alterations in head-group position *in situ* are also supported by the differences in the rates of charge recombination mediated by UQ_0 and MK_0, which will be addressed in detail in the following section. The large differences shown in Figure 9 for extensions from ethyl to pentyl and from pentyl to decyl may reflect differences in the *in situ* orientation of the quinone jointly established by the head group and components of the tail near the head group. These results indicate that the minimum *in situ* interaction free energies of the tail-substituted quinones at the Q_A and Q_B sites are established by an interplay between the quinone ring and the tail substituent.

5. Tail Structure Dependence of the Charge Recombination Kinetics. Comparison of data for many long-range biological electron transfers has shown that the reaction rates are determined principally by the following: (a) the electronic coupling, through the edge-to-edge distance between the donor and acceptor; (b) the reaction free energy; (c) the reorganization energy [Moser et al., 1992; for reviews of nonadiabatic electron-transfer theory, see DeVault (1984), Marcus and Sutin (1985), and Closs and Miller (1988)]. The rates of the BPh^- to Q_A and Q_A^- to $BChl_2^+$ electron transfers with substituted ubiquinone and menaquinone compounds as Q_A that are examined here are relatively insensitive to the reaction free energy and reorganization energy (Woodbury et al., 1985; Gunner et al., 1986; Gunner & Dutton, 1989; McComb et al., 1990). This is because the reaction free energies are within ~50 meV of the reorganization energy and the rate *versus* free energy dependence is shallow in the region around the reorganization energy (Gunner & Dutton, 1989; Moser et al., 1992). In addition, the reorganization energy, and the protein solvation contribution to the reaction free energy, are remarkably insensitive to dramatic changes in the head-group structure (Warncke & Dutton, 1993b). Changes in charge recombination induced by tail substitution are therefore determined primarily by changes in the distance-dependent electronic coupling.

The electron-transfer rate constant (k_{et}) decreases exponentially with increasing edge-to-edge separation distance (r) between the π-systems of the donor and acceptor beyond the van der Waals contact distance [r_0, taken as 3.6 Å for carbon atoms (Marcus & Sutin, 1985)]. The influence of the intervening medium on the distance-dependent decay of the electronic coupling is represented by the transmission coefficient, β. That the native isoprene tail might act as a preferred pathway from BPh^- to Q_A for the tunneling electron, thus providing a β value that is smaller than for transmission through the protein medium, is suggested by the X-ray crystallographic structures of the RC proteins from both *Rb. sphaeroides* (Allen et al., 1987) and *Rhodopseudomonas viridis* (Michel et al., 1986; Deisenhofer & Michel, 1989). In these structures the first four isoprene units of the native tail extend towards the BPh molecule, with the fourth unit of the tail in van der Waals contact with the farnesyl side chain of BPh. However, examination of the structure shows that the tail offers a circuitous route (33 *versus* 10 Å through the protein medium) involving 21 σ bonds and 1 through-space crossing at the point of van der Waals contact, thus making a preferred pathway of electron transmission along the tail very unlikely (Beratan et al., 1991). Moreover, the removal of the tail affects the physiologically nonproductive electron transfer from Q_A^- back to $BChl_2^+$ comparably, and the presence of a single isoprene unit substituent causes a 2.5-fold increase in the rate of Q_A^- to $BChl_2^+$ electron transfer without shortening the distance to BPh or $BChl_2$.

Therefore, the most simple explanation of the tail-induced increases in the rates of forward and reverse electron transfers is that the tail influences the distance between the donor and acceptor by altering the position of the quinone head group in the Q_A site. This is consistent with the interpretation of the differences in tail substitution effects on ubiquinone and menaquinone binding free energies in terms of altered *in situ* head-group positions. The changes in the charge recombination kinetics show that the dominant effects of the tail on head-group position are exercised by substitutions that interact with the binding region of the first isoprene unit. However, a second unit in the isoprene tail appears to lead to a small additional repositioning of the head-group, beyond that of the saturated tail structures. The adjustments of the native quinone ring appear to be complete with addition of the second isoprene unit, as shown by the absence of changes in rate with further isoprene additions. Assuming a β value of 1.4 $Å^{-1}$ (Moser et al., 1992), the ubiquinone and menaquinone head groups are relocated along the line connecting Q_A and $BChl_2$ by approximately 0.6 and 0.8 Å, respectively, after substitution with two isoprene units. The small effects of the tail on the rates have an insignificant influence on the efficiency of the physiological charge separation process in the RC protein.

6. Correlation of the Binding Free Energy Results with the RC Protein X-ray Crystallographic Structure. a. Extent of the Tail–Protein Interaction. Figure 10A shows a view of the native isoprene tail bound in the region of the Q_A site from the X-ray crystallographic structure of the *Rb. Sphaeroides*

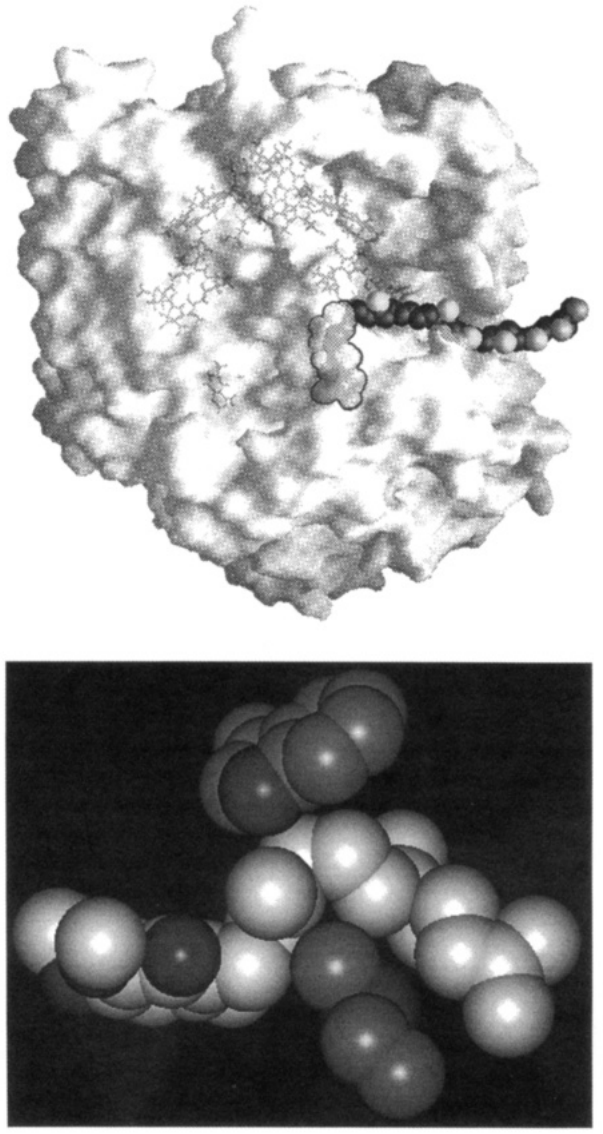

FIGURE 10: (A, top) Global aspect of the native tail of the Q_A site quinone derived from the X-ray crystallographic coordinates of the *Rb. sphaeroides* RC protein (Allen et al., 1987). (B, bottom) Ubiquinone head group and the first three isoprene units of the native tail with protein elements that are within 4 Å of the tail atoms of the first three isoprene units shown. The amino acid residues are methionine M218, methionine M256, and tryptophan M256.

RC protein (Allen et al., 1987). The first three isoprene units are surrounded by residues of the M subunit. Beginning with the last two or three carbon atoms of the third isoprene unit, tail units 4–6 are observed to protrude out of the M subunit and into a crevice between the membrane-spanning α-helices of the M and L subunits. There is no polypeptide element within a distance of 10 Å of isoprene units 4–10. Comparable observations are made for interaction of the native tail with protein at the Q_B site. The X-ray crystallographic structure thus corroborates the conclusions, based on the results presented in Figures 1–3, that the interaction of the tail with the protein interior at each site extends over only the first three isoprene units of the native tail.

b. Free Energetic Features Governing Quinone Binding Free Energies. Figure 10B shows the polypeptide atoms in the M-subunit Q_A site binding domain that are within the approximate van der Waals contact distance of 4 Å from the atoms composing the first three isoprene units of the native tail. There are apparently no specific, favorable enthalpic interactions of the π-electron systems in the isoprene double bonds with protein sulfur atoms or aromatic rings [e.g., see Burley and Petsko (1986)]. Methionine residues M218 and M256 contact the first two tail carbon atoms, and their position indicates that they oppose direct, linear extension of the tail from the head group. Therefore, these residues exercise the forces on tail binding that are resolved by the sequential ethyl- and propyl-substitution-induced decreases in affinity in the *n*-alkyl tail series, shown in Figure 9, as well as the loss in affinity for 2,3-diethyl- *versus* 2-ethyl-3-methyl-NQ shown in Figure 6. The fourth methylene carbon atom and the methyl group of the first isoprene unit interact with a relatively open region of the binding domain, in agreement with the favorable increment for propyl to butyl tail extension.

Further along the tail binding domain at the Q_A site, tryptophan M268 contacts the fifth, sixth, and seventh tail carbon atoms, and its position indicates that it opposes linear extension of the tail from the end of the first isoprene unit. This is demonstrated by the sharp twist of the second isoprene unit away from the first unit that is observed in the crystallographic structure. Thus, tryptophan M268 is a primary source of the unfavorable sequential contributions to affinity for *n*-alkyl tails with ≥ 5 carbon atoms. The steric constraint enforced by tryptophan M268 would also render accommodation of the 2,3-didecyl-1,4-naphthoqunone tail moiety energetically prohibitive, as confirmed by our inability to detect binding of this compound. Remarkably, molecular mechanical modeling of the interaction of the trienyl-UQ_2 tail with the Q_A site reveals that the rigid trienyl structure may be able to circumvent the block to direct extension at tryptophan M268. The trienyl tail is less bulky and shorter than alkyl analogs, and this may allow it to pass through a small opening to the side of the indole ring of tryptophan M268 and into a region which also contains a tightly bound molecule of the β-*n*-octyl glucoside detergent present during crystallization of the *Rb. sphaeroides* RC protein (Allen et al., 1987). These results provide a partial explanation for what appears to be, given the steric constraints observed for interaction of the native tail, an anomalously high affinity of the rigid trienyl-UQ_2 at the Q_A and Q_B sites.

In corroboration of the similar trends in tail-induced Q_A and Q_B site quinone binding free energy patterns observed in Figures 5 and 9, structural features comparable with those at the Q_A site are observed at the Q_B site. Residues valine L182, valine L220, and leucine L232 fulfill roles that correspond to those of M218, M256, and M268, respectively, at the Q_A site. The smaller bulk of these L-subunit amino acid side chains at the Q_B site may in part account for the apparently less restrictive nature of the Q_B tail binding domain relative to the Q_A site.

Features of the tail binding domain revealed in the RC protein structure are well-correlated with the free energetic features of the tail–protein interaction as revealed by the binding measurements. Comparable features of the tail–protein interaction are observed in the X-ray crystallographic structures of the RC proteins from *Rps. viridis* (Deisenhofer et al., 1985; Deisenhofer & Michel, 1989) and the *Rb. sphaeroides* structure of Schiffer and co-workers (Chang et al., 1986, 1991). In all of the RC proteins, strong steric constraints define the protein binding domain at each site and lead to a convoluted conformation for the first three isoprene units.

7. Origins of Site Specificity for Quinones Substituted with the Native Isoprene Tail Structure. Figure 11 shows the torsion potential energy for carbon–carbon single bonds in the first two isoprene units of the native tail compared with those for a model dimethyloctyl tail. Dihedral angles for bonds

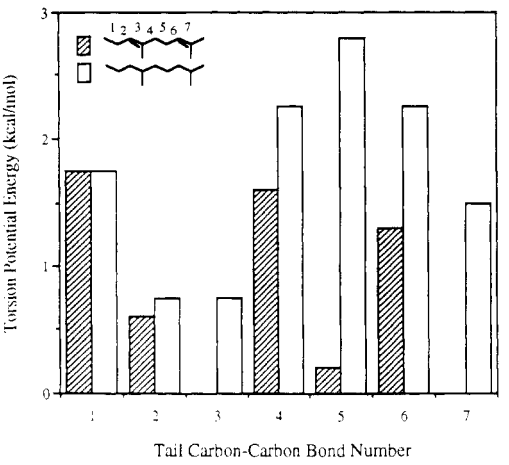

FIGURE 11: Torsion potential energy in Q_A site-bound di-isoprenyl and dimethyloctanyl tail structures as a function of carbon–carbon atom bond number. Values refer to the first two isoprene units of the native tail (shaded) and a model dimethyloctyl tail (open).

in the isoprene structure were obtained directly from the RC protein atomic coordinates (Allen et al., 1987), and the dihedral angles for the dimethyloctanyl tail are calculated from a model manipulated interactively to fit into the contours of the tail binding region displayed in the RC protein structure. Literature potential functions and maximum potential values (3.3 kcal/mol for bonds involving sp^3-hybridized carbon atoms and 2.0 kcal/mol for single bonds to sp^2-hybridized carbon) for hydrocarbons (Janz, 1967) were used to compute the torsion potential energy. Introduction of torsion potentials in the bound tail, as evidenced by the convoluted tail conformation *in situ*, leads to unfavorable contributions to the binding free energy. This is because the conformational energy of the tail is minimized in the extended, predominantly all-trans form that is present on average in solution. The integrated torsion potential energy calculated for the isoprene tail of UQ_2 is approximately 6 kcal/mol less unfavorable than that for the dimethyloctyl tail. This large difference is generated by the lowered barrier for rotations about bonds attached to sp^2 *versus* sp^3-hybridized carbon atoms and to the removal of two degrees of rotational freedom by the double bonds in the isoprene tail. The difference in computed torsional energy is larger than the observed difference in Q_A site affinity of 4 kcal/mol between UQ_2 and dimethyloctyl-UQ_0. This suggests that the two additional rotations in the saturated tail structure may allow it to relax into an energetically more favorable conformation than the one assumed for the calculations. These calculations indicate that differences in tail conformational energy in the protein-bound state make a dominant contribution to the experimentally observed specificity of the Q_A and Q_B sites for binding of quinones having isoprene *versus* saturated alkyl tail structures.

Contributions to the observed binding specificity from differences in unfavorable losses in solution entropy associated with restriction of the isoprene and dimethyloctyl tails in the protein site have been estimated using calculations based on statistical mechanical models of hydrocarbon chains (Person and Pimentel, 1953; Janz, 1967; Page and Jencks, 1971; Jencks, 1975). For both di-isoprenyl-UQ_0 and dimethyloctyl-UQ_0, the loss of free solution translational and rotational entropy is estimated to be 20 cal mol^{-1} K^{-1}, and the loss of internal rotational entropy in the tail moieties themselves is estimated to be 25 cal mol^{-1} K^{-1}, if it is assumed that the rotations are completely "frozen" *in situ*. The latter value may overestimate the rotational entropy loss, since the width of regions of the tail binding domain between the key steric constraints would appear to allow large-amplitude low-frequency motions in the tail that would offset unfavorable contributions to binding affinity due to losses of free solution entropy (Page & Jencks, 1971; Sturtevant, 1977). The estimated values for binding-induced entropy losses are comparable because the tail substituents are of similar mass and extent and because the higher rotational entropes contributed by single bonds adjacent to double bonds in the isoprene structure compensate for the negligible rotational entropy contributions from the double bonds. Therefore, although the absolute losses in tail entropy that are associated with binding appear to be significant, the relative difference between quinones carrying isoprene *versus* saturated alkyl substituents is negligible and thus does not contribute strongly to the observed binding specificity for the isoprene-substituted quinones. In contrast, entropy losses for the conjugated, rigid trienyl structure are estimated to be significantly smaller than for the isoprene and alkyl tails. This may partially account for the relatively high Q_A and Q_B site affinities for trienyl-UQ_2.

8. Role of the Tail–Protein Interaction in Quinone–RC Protein Binding In Vivo. The hexane solution binding results indicate that the native, 10-unit isoprene tail of UQ_{10} does not make a net favorable contribution to the binding free energy at either the Q_A or Q_B sites. Since the solvation environment in water-saturated hexane can be considered roughly analogous to that present in the hydrocarbon interior of the native bilayer membrane, this result suggests that the tail does not make a net favorable contribution to the strength of the *in vivo* quinone–protein interaction at the Q_A or Q_B sites. Further, the comparable trends in tail substitution-induced changes in quinone affinity at the Q_A and Q_B sites indicate that the nature of the interaction at each site is the same. Thus, the equilibrium interaction of the tail with the protein does not appear to contribute strongly to the different functional properties of the quinone at the Q_A and Q_B sites. However, the specificity displayed by each site for binding of the native isoprene tail structure is remarkable and is clearly related to the atomic structure of the RC protein at the Q_A and Q_B sites. In addition, the Q_A site discriminates strongly against quinones incorporating ortho-substituted dialkyl tails and does not accommodate hexane molecules, even when the RC protein is exposed to this solvent at molar concentrations. Thus, we propose that the principal role of the tail–protein interaction *in vivo* is to deter competitive inhibition of quinone interaction at each site by the hydrocarbon components of amphiphilic species dissolved in the membrane bilayer. These amphiphiles include not only the lipids of the photosynthetic membrane and their precursor and breakdown products but also carotenoids and other redox cofactors.

ACKNOWLEDGMENT

We thank R. Kaback for gifts of the isoprene-substituted ubiquinone and menaquinone compounds, K. M. Giangiacomo for help in the analysis of quinone binding at the Q_B site, D. Stevens and J. Haselgrove for assistance in the early analysis of the RC protein X-ray crystallographic structures, R. S. Farid for help with computer graphics, J. Deisenhofer and H. Michel for early communication of the atomic coordinates of the *Rps. viridis* RC protein, the laboratories of J. P. Allen, G. Feher, and D. C. Rees for early communication of the La Jolla group's *Rb. sphaeroides* RC protein atomic coordinates,

C.-H. Chang, J. Norris, and M. Schiffer for early communication of the Argonne group's *Rb. sphaeroides* RC protein atomic coordinates, and B. Honig and M. Lewis for use of their Silicon Graphics computer facilities.

REFERENCES

Allen, J. P., Feher, G., Yeates, T. O., Komiya, H., & Rees, D. C. (1987) *Proc. Natl. Acad. Sci. U.S.A. 84*, 5730–5734.

Beratan, D. N., Betts, J. N., & Onuchic, J. N. (1991) *Science 252*, 1285–1288.

Boxer, S. G. (1990) *Annu. Rev. Biophys. Biophys. Chem. 19*, 267.

Braun, B. S., Benbow, U., Lloyd-Williams, P., Bruce, J. M., & Dutton, P. L. (1986) *Methods Enzymol. 125*, 696–704.

Burley, S. K., & Petsko, G. A. (1986) *J. Am. Chem. Soc. 108*, 7995–8001.

Chang, C.-H., Tiede, D. M., Tang, J., Smith, U., Norris, J., & Schiffer, M. (1986) *FEBS Lett. 205*, 82–86.

Chang, C.-H., Ossama, E.-K., Tiede, D., Norris, J., & Schiffer, M. (1991) *Biochemistry 30*, 5352–5360.

Clayton, R. K., & Wang, R. T. (1971) *Methods Enzymol. 23*, 696–704.

Closs, G. L., & Miller, J. R. (1988) *Science 240*, 440–447.

Crane, F. L. (1977) *Annu. Rev. Biochem. 46*, 439–469.

Crofts & Wraight (1983) *Biochim. Biophys. Acta 726*, 149–185.

Deisenhofer, J., & Michel, H. (1989) *EMBO J. 8*, 2149–2170.

Deisenhofer, J., Epp, O., Miki, K., Huber, R., & Michel, H. (1985) *Nature 318*, 618–623.

DeVault, D. (1984) *Quantum Mechanical Tunneling in Biological Systems*, 2nd ed., Cambridge University Press, New York.

Diner, B. A., Schenck, C. C., & De Vitry, C. (1984) *Biochim. Biophys. Acta 766*, 9–20.

Ding, H., Robertson, D. E., Daldal, F., & Dutton, P. L (1992) *Biochemistry 31*, 3144–3158.

Dutton, P. L. (1986) in *Encyclopedia of Plant Physiology: Photosynthetic Membranes* (Staehlin, A., & Arntzen, C. J., Eds.) pp 197–237, Springer-Verlag, Berlin.

Feher, G., Allen, J. P., Okamura, M. Y., & Rees, D. C. (1989) *Nature 33*, 111–116.

Fersht, A. R. (1985) *Enzyme Structure and Mechanism*, Freeman, New York.

Giangiacomo, K. G. (1990) Doctoral Dissertation, University of Pennsylvania.

Giangiacomo, K. G., & Dutton, P. L. (1989) *Proc. Natl. Acad. Sci. U.S.A. 86*, 2658–2662.

Gunner, M. R. (1988) Doctoral Dissertation, University of Pennsylvania.

Gunner, M. R. (1991) *Curr. Top. Bioenerg. 16*, 319–367.

Gunner, M. R., & Dutton, P. L. (1989) *J. Am. Chem. Soc. 111*, 3400–3412.

Gunner, M. R., Liang, Y., Nagus, D. K., Hochstrasser, R. M., & Dutton, P. L. (1982) *Biophys. J. 37*, 226a.

Gunner, M. R., Braun, B. S., Bruce, J. M., & Dutton, P. L. (1985) in *Antennas and Pigments of Photosynthetic Bacteria* (Michel-Beyerle, M. E., Ed.) pp 298–305, Springer-Verlag, New York.

Gunner, M. R., Robertson, D. E., & Dutton, P. L. (1986) *J. Phys. Chem. 90*, 3783–3795.

Hansch, C., & Leo, A. (1979) *Substituent Constants for Correlation Analysis in Chemistry and Biology*, Wiley, New York.

Hederstedt, L., & Ohnishi, T. (1992) in *Molecular Mechanisms in Bioenergetics* (Ernster, L., Ed.) pp. 163–198, Elsevier, Amsterdam.

Janz, G. J. (1967) *Thermodynamic Properties of Organic Compounds*, Academic Press, New York.

Jencks, W. P. (1975) *Adv. Enzymol. 43*, 219–410.

Jencks, W. P. (1981) *Proc. Natl. Acad. Sci. U.S.A. 78*, 4046–4050.

Kirmaier, C., & Holten, D. (1987) *Photosynth. Res. 13*, 225–255.

Laing, Y., Nagus, D. K., Hochstrasser, R. M., Gunner, M. R., & Dutton, P. L. (1981) *Chem. Phys. Lett. 84*, 236–240.

Leo, A., Hansch, C., & Elkins, D. (1971) *Chem. Rev. 71*, 525–616.

Marcus, R. A., & Sutin, N. (1985) *Biochim. Biophys. Acta 811*, 265–322.

McComb, J. C., Stein, R. R., & Wraight, C. A. (1990) *Biochim. Biophys. Acta 1015*, 156–171.

McPherson, P. H., Okamura, M. Y., & Feher, G. (1990) *Biochim. Biophys. Acta 1016*, 289–292.

Michel, H., Epp, O., & Deisenhofer, J. (1986) *EMBO J. 5*, 2446–2451.

Mitchell, P. (1961) *Nature 191*, 144–148.

Mitchell, P. (1976) *J. Theor. Biol. 62*, 327–367.

Moser, C. C., & Dutton, P. L. (1987) *Biophys. J. 51*, 124a.

Moser, C. C., Keske, J. M., Warncke, K., Farid, R. S., & Dutton, P. L. (1992) *Nature 355*, 796–802.

Okamura, M. Y., Isaacson, R. A., & Feher, G. (1975) *Proc. Natl. Acad. Sci. U.S.A. 72*, 3491–3495.

Paddock, M. L., McPherson, P. H., Feher, G., & Okamura, M. Y. (1990) *Proc. Natl. Acad. Sci. U.S.A. 87*, 6803–6807.

Page, M. I., & Jencks, W. P. (1971) *Proc. Natl. Acad. Sci. U.S.A. 68*, 1678–1682.

Parot, P., Thiery, J., & Vermeglio, A. (1987) *Biochim. Biophys. Acta 893*, 534–543.

Parson, W. W. (1978) in *The Photosynthetic Bacteria* (Clayton, R. K., & Sistrom, W. R., Eds.) pp 455–469, Plenum, New York.

Person, W. B., & Pimentel, G. C. (1953) *J. Am. Chem. Soc. 75*, 532–540.

Prince, R. C., Halber, T. R., & Upton, T. H. (1988) in *Advances in Membrane Biochemistry and Bioenergetics* (Kim, C. H., Tedeschi, H., Diwan, J. J., & Salerno, J. C., Eds.) pp 469–477, Plenum Press, New York.

Robertson, D. E., Daldal, F., & Dutton, P. L. (1990) *Biochemistry 29*, 11249–11260.

Schelvis, J. P. M., Liu, B.-L., Aartsma, T. J., & Hoff, A. J. (1992) *Biochim. Biophys. Acta 1102*, 229–236.

Schönfeld, M., Montal, M., & Feher, G. (1980) *Biochemistry 19*, 1535–1542.

Sebban, P. (1988) *Biochim. Biophys. Acta 936*, 124–136.

Sharp, K. A., Nicholls, A., Friedman, R., & Honig, B. (1991) *Biochemistry 30*, 9686–9697.

Sturtevant, J. M. (1977) *Proc. Natl. Acad. Sci. U.S.A. 74*, 2236–2240.

Tanford, C. T. (1980) *The Hydrophobic Effect*, Academic Press, New York.

Warncke, K., & Dutton, P. L. (1993a) *Proc. Natl. Acad. Sci. U.S.A. 90*, 2920–2924.

Warncke, K., & Dutton, P. L. (1993b) *Biochemistry 32*, 4769–4779.

Warncke, K., Gunner, M. R., Braun, B. S., Yu, C.-A., & Dutton, P. L. (1987) *Prog. Photosynth. Res. 1*, 225–227.

Warncke, K., Gunner, M. R., Giangiacomo, K. M., Keske, J. M., Bruce, J. M., & Dutton, P. L. (1990) in *The Molecular Basis of Bacterial Metabolism* (Hauska, G., & Thauer, R., Eds.) pp 84–93, Springer-Verlag, Berlin.

Witt, H. T. (1979) *Biochim. Biophys. Acta 505*, 355–427.

Woodbury, N. W. T., Parson, W. W., Gunner, M. R., Prince, R. C., & Dutton, P. L. (1985) *Biochim. Biophys. Acta 851*, 6–22.

Wraight, C. A. (1979) *Photochem. Photobiol. 30*, 767–776.

Wraight, C. A., & Clayton, R. K. (1973) *Biochim. Biophys. Acta 333*, 246–260.

Yu, C.-A., Gu, L., Lin, Y., & Yu, L. (1985) *Biochemistry 24*, 3897–3902.